https://doi.org/10.15302/J-LAF-0-020040 Received Date | 2024-10-19 Accepted Date | 2025-03-19

Urban Flood Risk Prediction and Influencing Factors Analysis Based on the MaxEnt–PLUS Model

Bo LUAN[1,*], Jianing LUO[1], Xiulin YE[1], Weidong HUANG[2], Lu YU[2], Guangyu YU[2]

1 Green Infrastructure Institute, Peking University Shenzhen Institute, Shenzhen 518057, China
2 Urban Planning & Design Institute of Shenzhen, Shenzhen 518028, China

*CORRESPONDING AUTHOR
Address: No. 15 Gaoxin South 7th Road, Nanshan District, Shenzhen 518057, Guangdong Province, China
Email: luanbo@pku.edu.cn

GRAPHICAL ABSTRACT

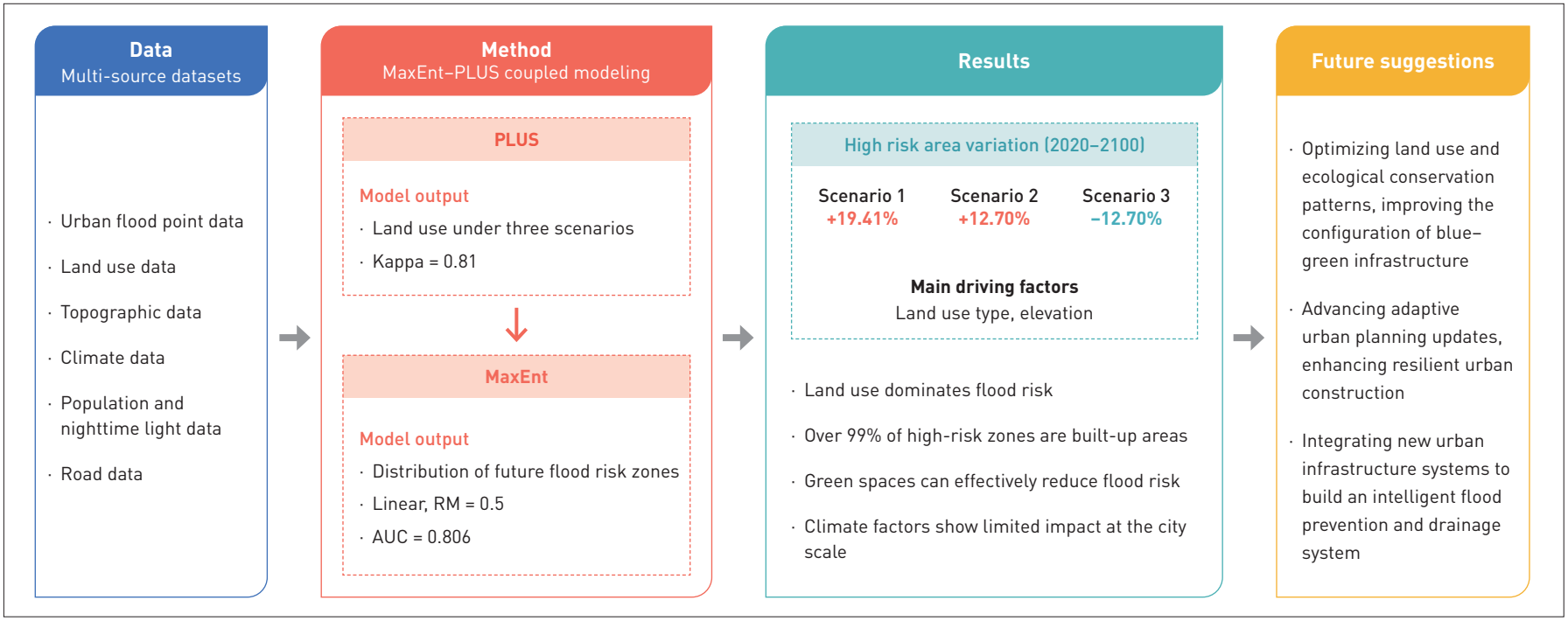

ABSTRACT

The scientific prediction of future urban flood risks has become a critical issue in urban planning. Shenzhen, a high-density city severely affected by typhoons, storm surges, and extreme rainfall, is facing escalating flood risks and urgently needs to enhance its urban resilience. This study couples the Maximum Entropy (MaxEnt) model with the PLUS model to forecast land use changes and urban flood risks in Shenzhen for the years 2040, 2060, 2080, and 2100 under business-as-usual, planning-guided, and ecological conservation scenarios, based on key factors derived from Global Climate Models (GCMs). This research further identifies the driving factors of flood risks and proposes strategies to optimize land use in urban renewal. The results indicate that built-up areas are exposed to significantly higher flood risks than blue and green spaces under the long-term trends of rising temperatures and precipitation. However, development under the ecological conservation scenario can effectively reduce urban flood risks, with the area of high-risk zones decreasing by 7.29% and low-risk zones increasing by 18.79% by 2100 compared with 2020. Meanwhile, land use type and elevation are identified as the main factors affecting flood risks. This research provides a scientific basis for enhancing resilience and optimizing green infrastructure in the context of urban renewal.

KEYWORDS

Urban Flood; MaxEnt–PLUS Model; Resilient City; Blue–Green Infrastructure; Climate Adaptation

HIGHLIGHTS

- Predicts future flood risks in Shenzhen under three development scenarios using the MaxEnt–PLUS model
- Under the business-as-usual scenario, built-up areas and corresponding flood risk are projected to increase substantially
- The expansion of green spaces can effectively reduce the area of high-risk urban flooding zones
- Land use type and elevation are the most influential factors contributing to flood risk

RESEARCH FUNDS

- Project of "Research on the Driving Mechanisms of Coastal Urban Green Space Resilience: A Case Study of the Guangdong–Hong Kong–Macao Greater Bay Area," National Natural Science Foundation of China (No. 52078004)
- Project of "Research and Development of Habitat Restoration and Ecological Resilience Technologies in Reservoir–River–Bay Systems," Shenzhen Science and Technology Program (No. KCXFZ20211020164205009)

EDITED BY Yuting GAO, Jiayi ZHOU

1 Background

The Intergovernmental Panel on Climate Change (IPCC) warns in its sixth assessment report that continued greenhouse gas concentration will lead to further increases in global surface temperature, with more frequent heavy precipitation and pluvial flood events[1]. Currently, China's urbanization is transitioning from rapid expansion to qualitative development. In many urban built-up areas, extensive impervious surfaces exacerbate the flood risk[2–3]. Shenzhen, a high-density coastal city in southern China, is highly exposed to climate-related hazards such as typhoons, storm surges, and extreme rainfall, resulting in escalating flood risk and an urgent need to enhance resilience[4–6]. The scientific prediction of future urban flood risk is fundamental for urban planning, disaster prevention, and the development of resilient and safe cities.

Urban flood risk assessment has emerged as a key research focus in recent years, commonly employing hydrological models, statistical models, and machine learning models. Hydrological models, e.g., the Storm Water Management Model (SWMM) and MIKE FLOOD model, simulate rainfall and drainage processes through physical mechanisms. However, these models require extensive high-resolution data and entail high computational complexity, limiting their applicability to future scenario simulations[7–8]. With the rise of data-driven methods, statistical and machine learning models have become prevalent in flood risk prediction. The Maximum Entropy (MaxEnt) model, rooted in information theory, is widely used in fields such as natural language processing, machine learning, and data mining. MaxEnt estimates the probability distribution with maximum entropy (i.e., the most uniform distribution) under known constraints, thereby preserving maximum uncertainty in the system[9]. Originally adopted for predicting species distributions in ecology based on occurrence data[10], MaxEnt has since been widely employed in biodiversity conservation and invasive species risk assessments. Owing to its small sample requirements and robust predictive performance, MaxEnt has gained traction in urban flood risk studies and has demonstrated promising accuracy. For instance, Wen Li et al. applied MaxEnt and Zonation models, along with six traditional machine learning models, to assess flood risk in Xi'an, China[11]. Similarly, Mohammad Eini et al. integrated MaxEnt with Genetic Algorithm to predict flood risk in Kermanshah, Iran, and found that MaxEnt outperformed Genetic Algorithm[12]. Peiting He et al. demonstrated that MaxEnt was more effective than the Random Forest (RF) model in identifying high flood risk zones[13]. However, current research on MaxEnt's parameter optimization and coupling application with other models remains limited.

Land use and land cover (LULC) change is a key driver of urban flood risk. Understanding and forecasting LULC dynamics and their effects on urban flood can support evidence-based urban planning[14–15]. Existing approaches include quantitative prediction models such as the Gray Forecasting Model (GFM), Markov Chain (MC) model, and System Dynamics (SD) model[16–18]; spatially explicit models such as Cellular Automata (CA), Conversion of Land Use and its Effects at Small Region Extent (CLUE-S), Future Land Use Simulation (FLUS), and Patch-generating Land Use Simulation (PLUS)[19–22]; as well as coupling models (e.g., Markov–CLUE-S, PLUS–SD)[23–25]. Among these, FLUS and PLUS have attracted attention for their algorithmic innovations and modeling flexibility.

FLUS uses adaptive CA and incorporates total land demand to simulate spatiotemporal land use changes driven by various factors, taking into account land use conflicts under multiple scenarios and emphasizing the integration of global land demand with localized transition probabilities[21]. For example, Xu Wang et al. employed FLUS to project ecological spatial dynamics in Hubei Province, China, providing policy guidance for future territorial planning and environmental protection[26]. However, FLUS typically trains on a dataset of a specific period, lacking the capacity to fully capture temporal dynamics and interactions among LULC drivers. By contrast, PLUS integrates the Land Expansion Analysis Strategy (LEAS) with the CA model based on multi-type Random Patch Seeds (CARS), which can simulate complex land use transitions, assign weightings to different driving factors, and support higher precision and faster computation for exploring refined spatial land use patterns[22]. Chen Li et al. indicated that PLUS better reflects the uncertainty and complexity of real-world land use transitions and yields higher simulation accuracy than other models[27]. While substantial progress has been made in FLUS- and PLUS-based LULC forecasting, studies coupling future urban development scenarios with long-term climate change impacts on flood risk remain relatively scarce. Jinyao Lin et al. and Nantao Xu et al. each coupled MaxEnt with FLUS to assess how different urban development scenarios affect future flood risks[28–29]. However, due to the uncertainties in long-term climate change and urban development trajectories, further investigation is needed to understand trends and drivers of flood risk.

This research takes Shenzhen as a case study and proposes an integrated urban flood risk prediction approach that combines the effects of climate change and land use transition. By constructing the coupled MaxEnt–PLUS model, it systematically assessed the long-term spatial evolution of urban flood risk under multiple future development scenarios and identified key influencing factors. The objective of this research is to provide a scientific basis for urban renewal in terms of land use adjustment, disaster prevention and emergency management, and infrastructure planning.

2 Study Area and Research Methods

2.1 Study Area

Shenzhen is located along the southern coast of Guangdong Province, China. It borders Daya Bay and Dapeng Bay to the east, the Pearl River Estuary and Lingdingyang Bay to the west, faces Hong Kong, China across the Shenzhen River to the south, and adjoins Dongguan and Huizhou to the north. The city experiences a subtropical monsoon climate, characterized by mild temperatures and abundant rainfall. Covering a total area of 1,997.47 km^2, Shenzhen has the highest population density among Chinese cities, reaching 8,806 people per square kilometer[30]. The city is frequently affected by typhoons, with historical records indicating an average of 3 to 4 typhoons occurring between July and September[31]. In recent years, the frequency of typhoons has shown an upward trend, accompanied by increasingly frequent extreme weather events, causing severe impacts and economic losses[32–33].

2.2 Data Sources and Preprocessing

2.2.1 Urban Flood Point Data

Urban flood point data were obtained from the *Special Plan and Implementation Scheme for Sponge City Construction in Shenzhen* (Optimized)[34]. To eliminate spatial autocorrelation effects in modeling and prediction, the dataset was preprocessed by Rstudio. This research first divided the study area into raster units with a spatial resolution of 30 m. In cases where multiple urban flood points fell within a single unit, only one point was randomly retained. After preprocessing, a total of 406 flood points were kept for analysis (Fig. 1).

2.2.2 Land Use Data

Land use data were sourced from the multi-period China's National Land Use and Cover Change (CNLUCC) dataset, provided by the Resource and Environmental Science Data Platform, for the years 2010 and 2020 (30 m spatial resolution). The dataset

Fig. 1 Distribution of urban flood points (after preprocessing) in Shenzhen, created based on the standard map No. Yue BS (2024) 031 from the Shenzhen Platform for Common Geospatial Information Services.

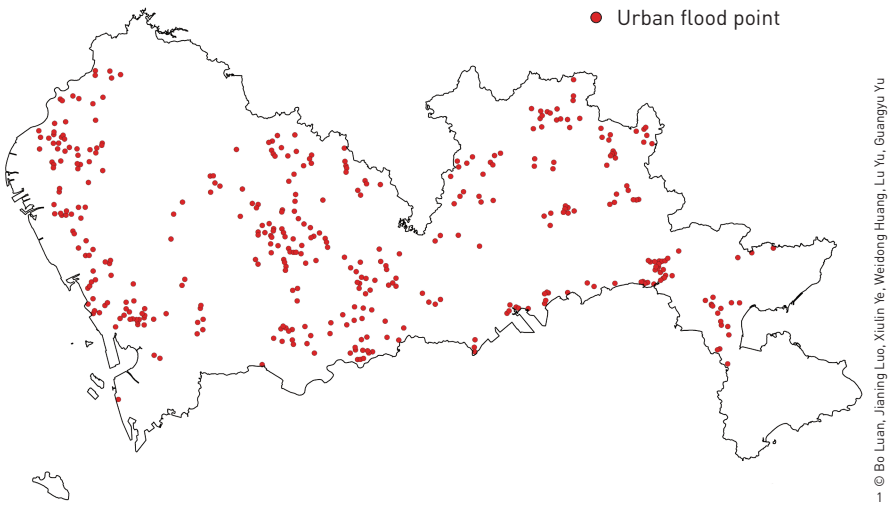

includes 6 land use categories—cultivated land, forest land, grassland, water body, urban/rural/industrial and mining/residential land, and marine area. Based on research needs, these categories were reclassified using ArcGIS 10.8 into consolidated land use types: green space (cultivated land, forest land, and grassland), blue space (water body), built-up area (urban/rural/industrial and mining/residential land), and marine area①. By extracting water bodies from land use data and generating raster data with the Euclidean Distance tool in ArcGIS 10.8, distance to water body was calculated (30 m resolution). The normalized difference vegetation index (NDVI) was obtained from the 2000–2022 China 30 m Annual Maximum NDVI Dataset, provided by the National Ecosystem Science Data Center (30 m resolution).

2.2.3 Topographic Data

The digital elevation models (DEMs) were obtained from the 2019 ASTER Global Digital Elevation Model Dataset (30 m resolution) via NASA Earthdata. Based on the DEMs, slope and surface roughness were derived using the Surface tools in ArcGIS 10.8.

2.2.4 Climate Data

The climate data of 2020 were sourced from the National Earth System Science Data Center (1 km resolution). Future climate data were obtained from the WorldClim database, which provides projections based on the Coupled Model Intercomparison Project Phase 6 (CMIP6). These projections include monthly mean minimum and maximum temperatures and precipitation derived from 23 Global Climate Models (GCMs), under 4 Shared Socioeconomic Pathways (SSPs)—SSP126 (low emissions), SSP245 (moderate emissions), SSP370 (medium–high emissions), and SSP585 (high emissions). Among these, SSP245 that reflects potential climate changes under current or moderate policy interventions and was selected for analysis in this research[35]. For climate modeling, the BCC-CSM2-MR model developed by Beijing Climate Center was adopted due to its high accuracy in simulating tropospheric temperature and circulation in East Asia monsoon regions[36]. This model includes projections for 4 time periods (2021–2040, 2041–2060, 2061–2080, and 2081–2100). All climate data were interpolated to a 30 m resolution for refined spatial analysis.

① In coastal regions, some present-day land was created through reclamation. Therefore, "marine area" appeared as a distinct land use type. This category was excluded from future development scenarios where land reclamation is no longer considered.

2.2.5 Population and Nighttime Light Data

Population data (2020, resolution of 100 m) were downloaded from the dataset shared on Figshare by Yuehong Chen's research team from Hohai University. Nighttime light data, specifically the radiance values at the year of 2020 with the resolution of 500 m, were sourced from the Harvard Dataverse. The data were then interpolated to generate raster data with a spatial resolution of 30 m.

2.2.6 Road Data

The road data were sourced from OpenStreetMap. This research further created raster data of distance to various road classes with the Euclidean distance tool in ArcGIS 10.8, with a spatial resolution of 30 m.

2.3 Research Models and Methods

Using the PLUS model, this research simulated the future land use patterns under various urban development scenarios. Based on current urban flood point data, the MaxEnt model was used to predict the spatial distribution of flood risk under climate change. Coupling the MaxEnt and PLUS models enables the identification and assessment of long-term flood risk trends across different development pathways, providing a scientific basis for urban planning.

2.3.1 PLUS Model

The PLUS model is an advanced tool developed in recent years to simulate land use changes based on a patch-generating mechanism. It is particularly well-suited for analyzing land use dynamics and urban expansion under complex development scenarios[22]. This research incorporated 10 driving factors into the PLUS model, including natural factors (i.e., elevation, slope, surface roughness, annual mean temperature, annual precipitation, and NDVI) and socioeconomic factors (i.e., population density, nighttime light, distance to road, and distance to water body). Using the LEAS module in PLUS, an RF algorithm was employed to identify the key drivers for the expansion of each land use type and calculate the likelihood that each type of land use would be developed[37]. The LEAS module works by extracting the expansion zones between two land use periods; thus, changes between 2010 and 2020 were used to calculate spatial dynamics (Fig. 2). The land use projection was conducted with the CA model that integrates both top-down mechanisms (i.e., total land use demand) and bottom-up mechanisms (i.e., land use conflicts). An adaptive inertia coefficient was applied to adjust the impact of land use demand on local spatial competition, ensuring consistency between simulated land

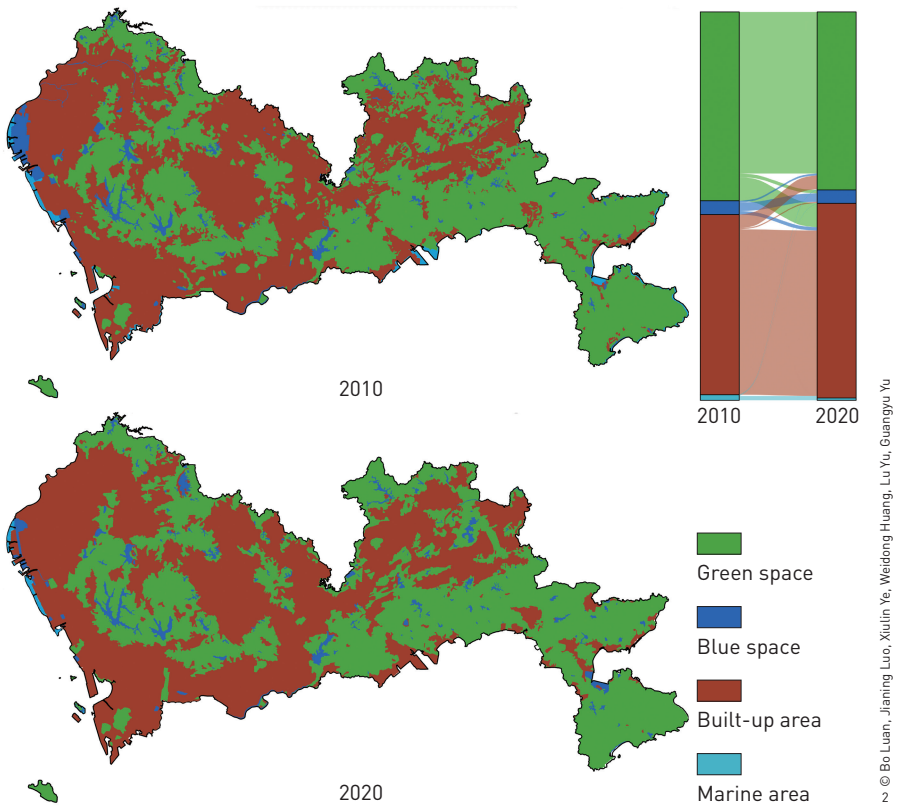

Fig. 2 Land use patterns and changes in Shenzhen (2010–2020), created based on the standard map No. Yue BS (2024) 031 from the Shenzhen Platform for Common Geospatial Information Services.

expansion and predefined demand targets.

To simulate urban development scenarios under different planning strategies in the PLUS model, the number of units allocated to each land use type was adjusted under each scenario using land use transition probabilities. Based on Shenzhen's current conditions, this research designed three scenarios and projected land use distributions for the years 2040, 2060, 2080, and 2100.

1) Business-as-usual scenario (Scenario 1). Using 2020 as the base year, apply the MC model to forecast land use changes, leveraging the land use change rates and development potential reflected in the driving factors from 2010 to 2020, regardless of the planning policy constraints.

2) Planning-guided scenario (Scenario 2). In accordance with the *Shenzhen Territorial Spatial Ecological Protection and Restoration Plan* (2021–2035), set the transition probabilities as follows: blue spaces remain unchanged, and the probability of green spaces converting to built-up areas increases by 1% per decade.

3) Ecological conservation scenario (Scenario 3). Accounting for potential urban shrinkage under population decline, reduce construction land for ecological conservation. Building upon Scenario 1, reduce the probability of green spaces converting to built-up areas by 50% and increase the probability of built-up areas reverting to green spaces by 10% every decade, while blue spaces remain unchanged[38].

2.3.2 MaxEnt Model

This research constructed the MaxEnt model with the spatial distribution of observed urban flood points and related hazard-inducing factors to evaluate the contribution of each factor to the occurrence of flood events and to estimate the potential distribution of future urban flood. The performance of the MaxEnt model was then assessed using the Receiver Operating Characteristic (ROC) curve and the Area Under the ROC Curve (AUC).

Previous studies have identified temperature, precipitation, topography, and land use as primary influencing factors for flood events[39–45]. Accordingly, this research incorporated three categories of influencing factors as predictors in the MaxEnt model, including meteorological factors, topographic factors (i.e., elevation, slope, surface roughness), and land use type. Given that urban flood in Shenzhen mainly occurs during the hot and rainy season, 9 factors from GCMs were selected as candidate meteorological factors (Table 1). These factors were further filtered to reduce multicollinearity and ensure model robustness through correlation analysis and permutation importance assessment. As a result, annual mean temperature and annual precipitation were kept as the final meteorological factors.

Table 1: Meteorological factors selected from GCMs

Code	Meteorological factor
Bio1	Annual mean temperature
Bio5	Max temperature of warmest month
Bio8	Mean temperature of wettest quarter
Bio10	Mean temperature of warmest quarter
Bio12	Annual precipitation
Bio13	Precipitation of wettest month
Bio15	Precipitation seasonality
Bio16	Precipitation of wettest quarter
Bio18	Precipitation of warmest quarter

In summary, six variables were included in the final MaxEnt model: annual mean temperature, annual precipitation, elevation, slope, surface roughness, and land use type. To prevent overfitting due to MaxEnt's default settings and to improve model interpretability[46–47], parameter tuning was conducted using the ENMeval package[48]. It involved combining feature classes (FCs), i.e., linear (L) and linear + quadratic (LQ), and regularization multipliers (RMs) ranging from 0.5 to 4.0 (in 0.5 increments), resulting in 16 candidate models. The highest AUC (0.806) was achieved with the combination of L and RM = 0.5, which was selected as the optimal configuration for flood risk prediction. To further reduce spatial autocorrelation and improve model validation, the research applied block partitioning to divide the study area into four regions (Fig. 3) for spatially independent testing[48].

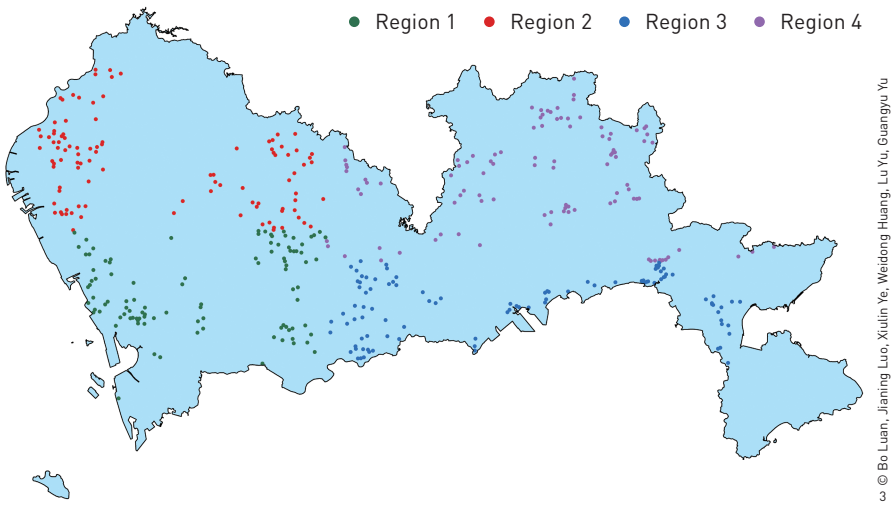

Fig. 3 Block partitioning of urban flood points using ENMeval, created based on the standard map No. Yue BS (2024) 031 from the Shenzhen Platform for Common Geospatial Information Services.

3 Results and Discussion

3.1 Land Use Changes Under Different Development Scenarios

Based on the PLUS model, the simulated land use under the three development scenarios is illustrated in Figs. 4 and 5. In 2020, the coverages of built-up areas, green spaces, and blue spaces in Shenzhen were 1,009.32 km^2, 922.90 km^2, and 65.25 km^2, respectively. Under Scenario 1, continuous urban expansion is

Fig. 4 Simulated land use changes in Shenzhen under different scenarios, created based on the standard map No. Yue BS (2024) 031 from the Shenzhen Platform for Common Geospatial Information Services.

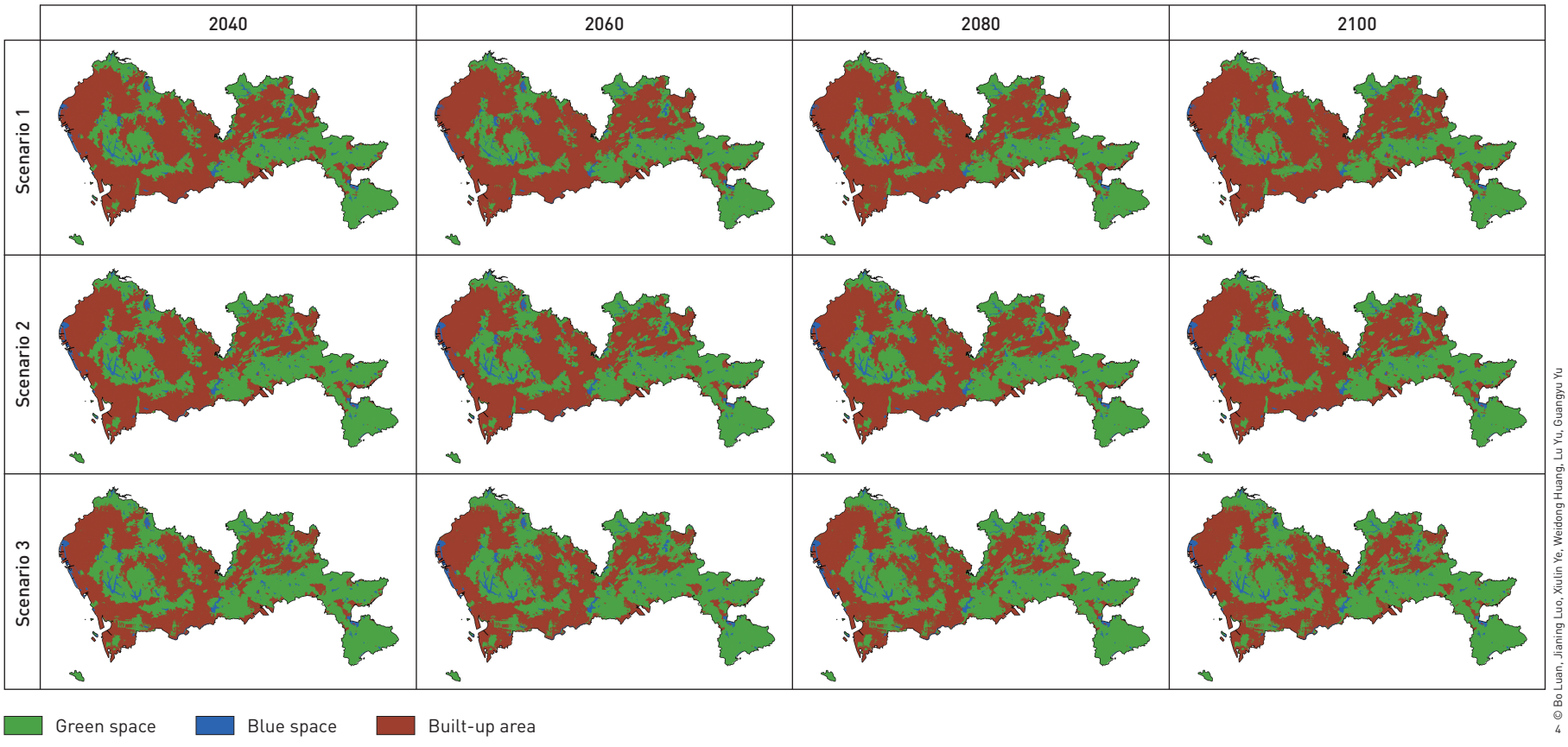

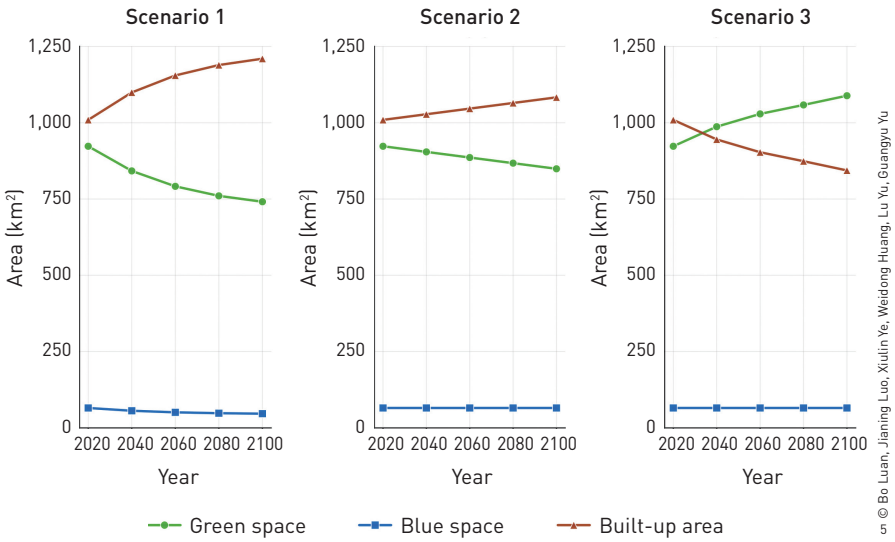

Fig. 5 Simulated land use area changes in Shenzhen under different scenarios.

observed, with built-up areas increasing to 1,209.83 km² by 2100 (19.87% increase compared with 2020). Meanwhile, green spaces and blue spaces shrink to 741.09 km² and 46.56 km², representing decreases of 19.70% and 28.64%, respectively. Under Scenario 2, blue spaces remain unchanged, while built-up areas increase to 1,083.16 km² by 2100, showing a growth of 7.32%; while green spaces decrease to 849.06 km², marking an 8.00% reduction. In contrast, under Scenario 3, blue spaces are also preserved, green spaces recover to 1,088.53 km² by 2100, presenting a 17.95% increase from 2020, and built-up areas reduce to 843.69 km², showing a decline of 16.41%.

A trade-off trend is evident between land use types, as indicated by the ratio of built-up areas to green spaces, which was 1.09 in 2020. As the projection period extends, the ratio disparity among the three scenarios becomes more pronounced. In 2040, the ratios under Scenarios 1, 2, and 3 are 1.31, 1.14, and 0.96, respectively. By 2100, the gap widens further, with ratios of 1.63, 1.28, and 0.78. Under Scenario 1, the built-up areas reach 1.12 times (2040) and 1.43 times (2100) that of Scenario 2. Given the limited initial area, blue spaces in Shenzhen experience a slight absolute reduction under Scenario 1 (Fig. 4).

According to the ranking of factor contributions, among the 10 driving factors used in the PLUS model, distance to road and nighttime light are the two most critical in driving changes in built-up areas and green spaces. The contribution of distance to road to area changes of built-up areas and green spaces is 25.8% and 15.9%, respectively, while that of nighttime light in built-up areas and green spaces is 15.9% and 11.5%, respectively. This indicates that socioeconomic factors exert a stronger influence on land use change in Shenzhen than natural factors.

The accuracy of the PLUS model is assessed using the Kappa coefficient. A Kappa coefficient between 0.6 and 0.8 indicates high consistency in the simulation results, while a coefficient greater than 0.8 signifies near-perfect agreement[49]. In this research, the Kappa coefficient reaches 0.81, with an overall accuracy of 0.90, demonstrating high reliability of the model's predictions.

3.2 Flood Risk Projections From 2040 to 2100 Under Different Scenarios

Future land use data generated by the PLUS model across the years 2040, 2060, 2080, and 2100 were input into the MaxEnt model to predict future flood risks. Following the classification approach by Sahar Rezaei et al.[50], flood risk was divided into three levels: high risk (probability > 0.6), medium risk (0.3 < probability ≤ 0.6), and low risk (0 ≤ probability ≤ 0.3). The results (Fig. 6) show that future high-risk zones are mainly concentrated in the densely built-up areas in western, southwestern, southern, and northern Shenzhen. Most of the eastern peninsula remains in low-risk zones, consistent with findings by Jinyao Lin et al.[28].

Changes in flood risk zones in Shenzhen from 2040 to 2100 under different development scenarios are shown in Fig. 7. Under Scenario 1, the area of low-risk zones declines from 967.19 km² in 2020 to 825.81 km² in 2100, a reduction of 14.62%. Medium-risk areas exhibit slight fluctuations, generally maintaining around 300 km². The high-risk zones, measuring 731.52 km² in 2020, show a steady upward trend, increasing to 786.82 km² by 2040, a 7.56% increase from 2020, and reaching 873.52 km² by 2100, a 19.41% increase from 2020. Under Scenario 2, the low-risk zones show a slight downward trend, decreasing to 923.90 km² by 2100, a 4.48% reduction from 2020. Medium-risk zones show an overall downward trend, from 298.75 km² in 2020 to 249.11 km² in 2100, a 16.62% decrease. High-risk zones display a fluctuating upward trend, peaking at 824.46 km² in 2100, representing a 12.70% increase from 2020. Under Scenario 3, the area of low-risk zones increases, reaching 1,027.66 km² in 2040, a 6.25% increase from 2020, and further expanding to 1,148.91 km² by 2100, an 18.79% increase from 2020. The high-risk zones fluctuate downward, reaching a temporary peak of 709.01 km² in 2060, before stabilizing at 670.62 km² and 678.22 km² in 2080 and 2100, respectively.

Overall, from 2020 to 2100, high-risk zones in Shenzhen exhibit a fluctuating trend. Under Scenarios 1 and 2, high-risk zones increase between 2040 and 2060, decrease between 2060 and

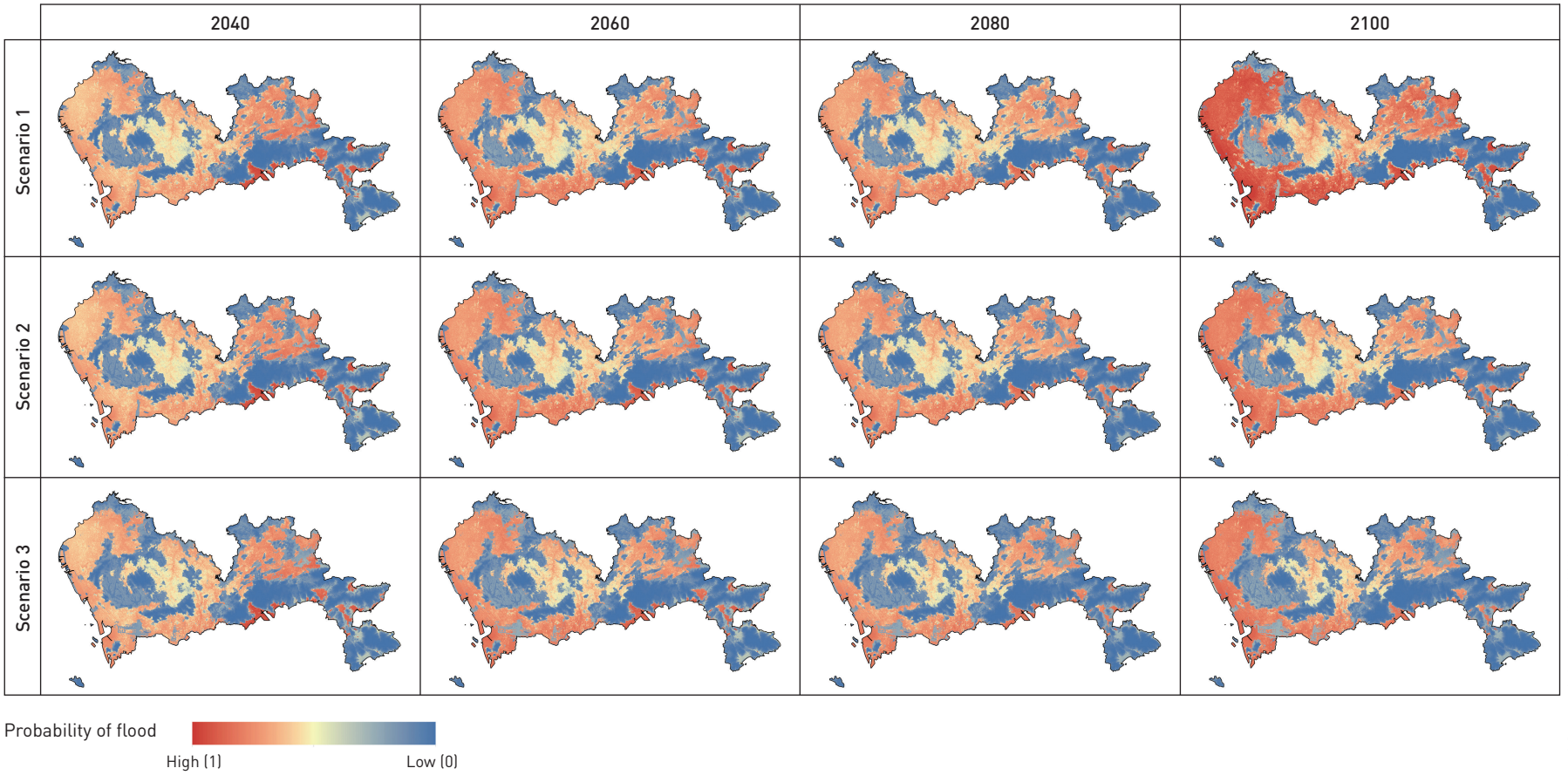

Fig. 6 Spatial distribution of flood risk zones in Shenzhen under different scenarios, created based on the standard map No. Yue BS (2024) 031 from the Shenzhen Platform for Common Geospatial Information Services.

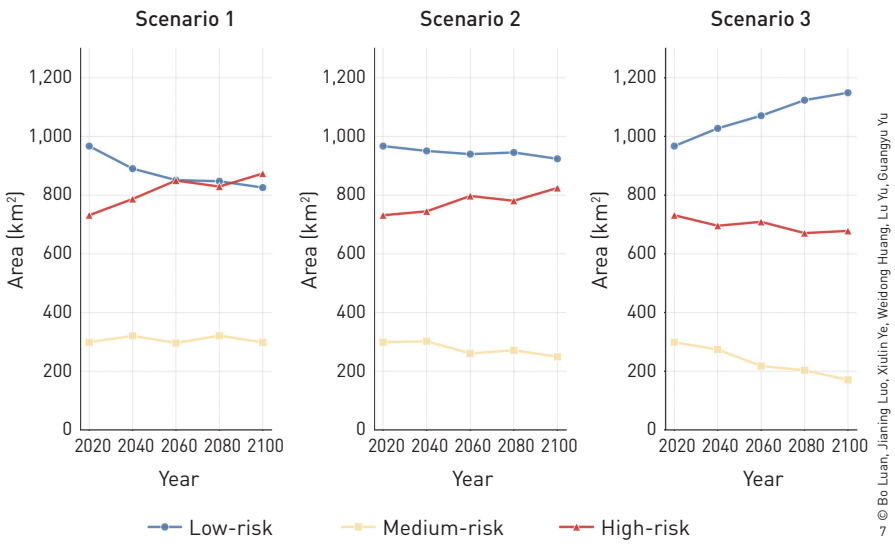

Fig. 7 Area changes in different levels of flood risk zones in Shenzhen under different scenarios.

2080, and peak again by 2100. Under Scenario 3, however, high-risk zones exhibit a general decline. This long-term trend suggests that if Shenzhen continues its development as Scenarios 1 and 2, urban flood risk will intensify. In contrast, ecological conservation efforts could substantially reduce urban flood risks.

3.3 Land Use Type Analysis Within Flood Risk Zones

Table 2 presents a comparative analysis of land use types within flood risk zones under different scenarios in 2040 and 2100. In 2020, the total area of high-risk zones was 731.53 km^2, almost entirely consisting of built-up areas. In 2040 and 2100, across all three scenarios, built-up areas account for 99.99% of high-risk zones. In 2020, medium-risk zones were also dominated by built-up areas, which occupied 89.44% of these areas. By 2040, the shares of built-up areas in medium-risk zones are 92.04%, 90.02%, and 88.25% under Scenarios 1, 2, and 3, respectively. By 2100, these proportions rise to 98.15%, 97.55%, and 94.62%. In contrast, low-risk zones were primarily composed of green spaces, which accounted for 92.15% in 2020. By 2040, green spaces make up 91.71% to 92.91% of low-risk zones across the three scenarios. By 2100, this share ranges from 89.07% to 93.95%.

In summary, high-risk zones are composed almost entirely of built-up areas, medium-risk zones are dominated by built-

Table 2: Area changes of land use types within flood risk zones under different scenarios (unit: km^2)

Flood risk zone	Land use type	2020	2040			2100		
			Scenario 1	Scenario 2	Scenario 3	Scenario 1	Scenario 2	Scenario 3
High-risk	Green space	0.07	0.07	0.07	0.07	0.01	0.01	0.01
	Blue space	0.00	0.00	0.00	0.00	0.00	0.00	0.00
	Built-up area	731.46	786.75	744.77	695.68	873.51	824.45	678.21
	Total	731.53	786.82	744.84	695.75	873.52	824.46	678.22
Medium-risk	Green space	31.56	25.49	30.12	32.20	5.52	6.11	9.17
	Blue space	0.00	0.00	0.00	0.00	0.00	0.00	0.00
	Built-up area	267.19	294.83	271.77	241.86	292.62	243.00	161.17
	Total	298.75	320.32	301.89	274.06	298.14	249.11	170.34
Low-risk	Green space	891.27	816.55	874.26	954.78	735.55	842.94	1,079.35
	Blue space	65.25	56.15	65.25	65.25	46.56	65.25	65.25
	Built-up area	10.67	17.63	11.23	7.63	43.70	15.71	4.31
	Total	967.19	890.33	950.74	1,027.66	825.81	923.90	1,148.91

up areas, and low-risk zones consist mainly of green and blue spaces. This spatial pattern highlights a significant difference in flood vulnerability across land use types under long-term climate change—built-up areas are more susceptible to flood risk compared with blue and green spaces.

3.4 Analysis of Influencing Factors of Flood Risk

This research employs the MaxEnt model to investigate the relationships between various hazard-inducing factors and the probability of urban flood. The model yielded an AUC of 0.806, indicating high accuracy (AUC > 0.6)[51].

Figure 8 illustrates the effects of different influencing factors on flood probability. Specifically, flood risk decreases sharply when annual average temperature rises from 21.9°C to 24.0°C, while remaining relatively stable at both ends. In contrast, flood risk increases linearly with annual precipitation, as greater rainfall leads to increased surface runoff and, consequently, a higher probability of flood. For topographic factors, flood probability decreases significantly with increasing slope and elevation, as low-lying, flat terrains tend to drain poorly and are more prone to urban flood[52–53]; flood probability increases with surface roughness, as elevated areas can disrupt runoff pathways and depressions might impede drainage efficiency, leading to longer and deeper water accumulation[54]. Regarding land use type, built-up areas exhibit the highest flood risk probability (0.64), while green spaces (0.18) and blue spaces (0.11) show relatively low probabilities.

As shown in Fig. 9, among the 6 influencing factors, land use type holds the highest permutation importance (50.78%), followed by elevation (33.48%), indicating these factors contribute the most to flood risk. This finding aligns with previous research[29,55]. Although under the SSP245 scenario, Shenzhen's annual average temperature is projected to increase by approximately 1°C between 2040 and 2100, and annual precipitation shows a general upward trend, aside from fluctuations in 2080 (Fig. 10), this research finds that meteorological factors have relatively low contributions to flood risk (each with permutation importance

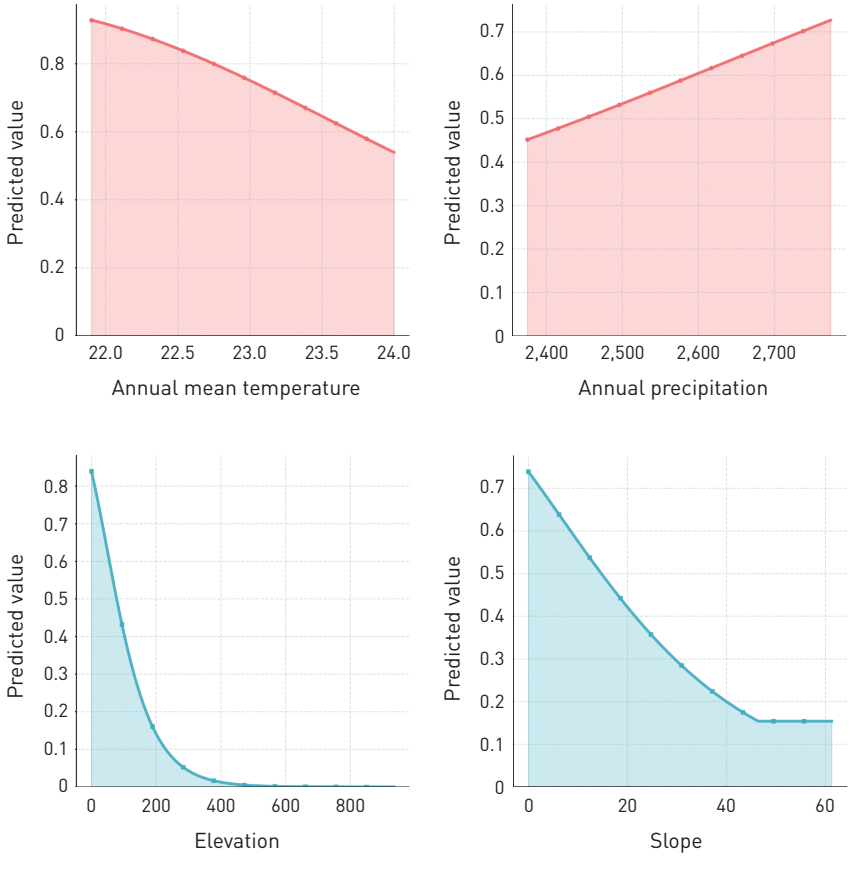

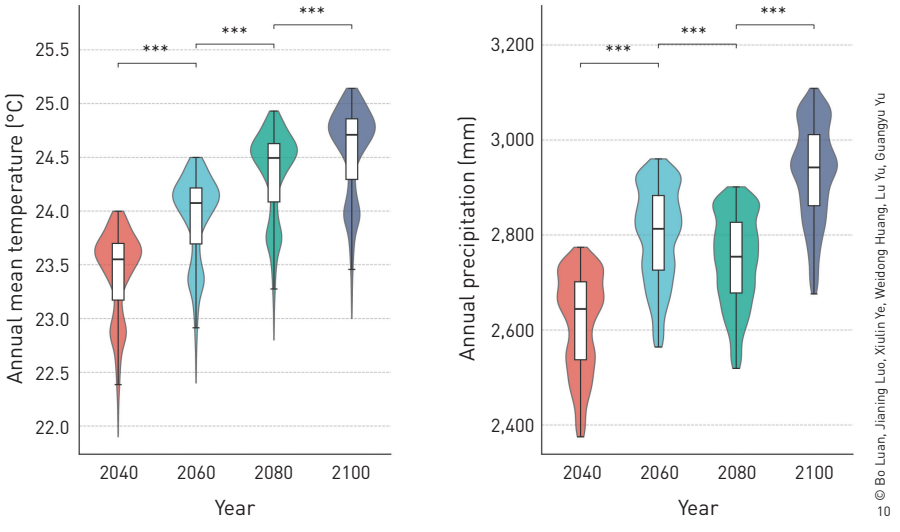

Fig. 8 The effects of different influencing factors on flood probability.
Fig. 9 Permutation importance results of flood risk influencing factors.
Fig.10 Annual mean temperature and annual precipitation projection under SSP245 scenario.

below 10%). This is likely due to the relatively small spatial variability of meteorological factors (rainfall and temperature) at the city scale, while land use and topography show significant spatial heterogeneity. For instance, average annual precipitation in eastern Shenzhen is 2,070 mm, compared with 1,955 mm in the west—a difference of only about 5%. However, the proportion of built-up areas in the west is 60.26%, which is 1.62 times that in the east (27.25%). Furthermore, the average elevation in the east is 114.9 m, which is 2.23 times that in the west. Ultimately, it shapes the urban flood pattern in Shenzhen—higher risk in the west, lower in the east.

3.5 Strategic Recommendations

Based on the flood risk projections, land use type stands out as the dominant influencing factor shaping the spatial distribution of flood risk, whereas meteorological factors primarily amplify the existing level of risks rather than directly determine them. Therefore, Shenzhen should develop flood risk management strategies aligned with its future urban development scenarios to reduce the risks brought by the uncertainties of climate change through the following approaches.

1) Optimize land use and ecological conservation patterns and improve blue–green infrastructure development. In response to Shenzhen's ongoing urban transformation and renewal, the green and blue spaces should be expanded, and development in low-lying flood-prone areas should be avoided. Improvements should be made to green infrastructure, such as green roofs, sunken gardens,

and permeable pavements. A comprehensive upgrade to sponge city systems should be promoted to enhance rainfall absorption and water resource utilization in high-density built-up areas. Furthermore, flood peak regulation and water discharge capacities of rivers and wetlands should be enhanced. For projected high- and medium-risk flood zones, phased implementation of blue–green infrastructure upgrades and green space expansion should be pursued to enhance the resilience of the city.

2) Advance adaptive urban planning to build a more resilient city. Spatial planning should incorporate mandatory constraints of land use and allow for adaptive flexibility to accommodate both possible quantitative and qualitative development scenarios. In high-density built-up areas, urban renewal should integrate adaptive strategies such as high-quality sponge city initiatives and decentralized rainwater management technologies at the neighborhood/block levels.

3) Integrate new urban infrastructure to build an intelligent flood management system. Leveraging digital and smart technologies, new urban infrastructure should be deeply integrated with blue–green infrastructure to achieve precise monitoring, timely response, and efficient control of urban flood disasters. A smart drainage system can be developed by integrating remote sensing, unmanned aerial vehicles, Internet of Things (IoT) sensors, and automated control technologies. In addition, flood early warning systems can be established using big data, artificial intelligence, and deep learning to rapidly and accurately predict flood areas and their severity during extreme rainfall events. A comprehensive emergency response platform based on IoT and big data should also be constructed to enable quick and effective coordination and deployment of emergency resources.

4 Conclusions and Prospects

Based on GCM-derived influencing factors, this research integrates the MaxEnt and PLUS models to project the future urban flood risk in Shenzhen under three development scenarios. The main conclusions are as follows.

1) The simulation of urban expansion shows that under Scenario 1, built-up areas expand significantly while green and blue spaces shrink considerably. Under Scenario 2, built-up areas grow moderately with a slight reduction in green spaces. In contrast, Scenario 3 shows the opposite trend, with a marked increase in green spaces and a corresponding reduction in built-up areas. By 2100, the ratio between built-up areas and green spaces differs significantly across scenarios: 1.63 under Scenario 1 and only 0.78 under Scenario 3. Socioeconomic factors are identified as the primary drivers of land use change.

2) In the context of long-term climate trends characterized by rising temperatures and increasing precipitation, Shenzhen will have a broader extent of high-risk zones if it follows the current development pathway driven by built-up area expansion. In contrast, promoting ecological conservation and relative land expansion can effectively reduce urban flood risk.

3) Urban flood risk is closely tied to land use patterns and spatial characteristics—land use type and elevation are two pivotal factors contributing to flood risk. High-risk flood areas in Shenzhen are primarily concentrated in built-up areas, whereas green and blue spaces account for the highest proportion in low-risk areas. Blue spaces, in particular, are entirely located within low-risk zones. Under the long-term influence of climate change, built-up areas are more vulnerable to flood risks than green and blue spaces.

4) Shenzhen should formulate proactive flood risk management strategies based on future development scenarios. This includes optimizing land use and ecological conservation patterns, improving the configuration of blue–green infrastructure, advancing adaptive urban planning updates, enhancing resilient urban construction, and integrating new urban infrastructure systems to build an intelligent flood prevention and drainage system.

This research provides a scientific basis for building resilient cities and supports flood risk management and blue–green infrastructure planning. However, several issues can be further investigated. First, the long-term projections in this research are based on land use data from 2010 and 2020, which may lead to forecasting biases for future urban transformation, with longer prediction periods introducing larger uncertainties. Second, the MaxEnt model in this research employs GCM-based meteorological factors with relatively low spatial resolution for flood risk prediction, which is suitable for global-scale studies rather than city-scale assessments. Future studies may incorporate deep learning methods to enhance the precision of climate models and integrate critical factors such as urban drainage networks and micro-topographic variations to improve predictive accuracy.

ELECTRONIC SUPPLEMENTARY MATERIAL

Supplementary material is available in the online version of this article at https://doi.org/10.15302/J-LAF-0-020040.

Competing interests | The authors declare that they have no competing interests.

REFERENCES

[1] Intergovernmental Panel on Climate Change. (2021). *Climate Change 2021: The Physical Science Basis. Contribution of Working Group I to the Sixth Assessment Report of the Intergovernmental Panel on Climate Change*. Cambridge University Press.

[2] Li, X., & Kuang, W. (2020). Urban land use/cover change and its impact on urban flood regulation ecosystem service in Beijing. *Acta Ecologica Sinica*, *40*(16), 5525–5533.

[3] Zhang, H., Yin, Z., Yin, J., An, Y., & Zhang, S. (2011). Vulnerability assessment of urban rainstorm water-logging in Pudong of Shanghai in terms of land use. *Journal of Shanghai Normal University (Natural Sciences)*, *40*(4), 427–434.

[4] Luan, B., Liu, Y., Che, D., Zhou, W., Hu, L., & Lin, Y. (2024). Exploring nature-based solutions on refined waterbird habitats restoration in high-density urban area: A case study of the Futian Mangrove National Important Wetland in Shenzhen, China. *Landscape Architecture Frontiers*, *12*(3), 36–52.

[5] Luan, B., Ding, R., Wang, X., & Zhu, M. (2020). Exploration of resilient design paradigm of urban green infrastructure. *Landscape Architecture Frontiers*, *8*(6), 94–105.

[6] Qi, X., Luan, B., Zhou, W., Luo, J., & Yu, L. (2025). Factors influencing urban coastal ecological resilience based on the STIRPAT model: A case study of Shenzhen City. *China Environmental Science*, *45*(1), 416–429.

[7] Rossman, L. A. (2010). *Storm water management model user's manual, Version 5.0*. U.S. Environmental Protection Agency.

[8] DHI Water & Environment. (2017). *MIKE FLOOD: 1D-2D modelling user manual.*

[9] Sepúlveda-Fontaine, S. A., & Amigó, J. M. (2024). Applications of entropy in data analysis and machine learning: A review. *Entropy*, *26*(12), 1126.

[10] Phillips, S. J., & Dudík, M. (2008). Modeling of species distributions with Maxent: New extensions and a comprehensive evaluation. *Ecography*, *31*(2), 161–175.

[11] Li, W., Jiang, R., Wu, H., Xie, J., Zhao, Y., Li, F., & Gan, T. Y. (2024). An integrated urban flooding risk analysis framework leveraging machine learning models: A case study of Xi'an, China. *International Journal of Disaster Risk Reduction*, *112*, 104770.

[12] Eini, M., Kaboli, H. S., Rashidian, M., & Hedayat, H. (2020). Hazard and vulnerability in urban flood risk mapping: Machine learning techniques and considering the role of urban districts. *International Journal of Disaster Risk Reduction*, *50*, 101687.

[13] He, P., Liu, D., Lu, S., He, X., Li, H., Yang, L., & Lin, J. (2022). Influencing factors of waterlogging and waterlogging risks in Shenzhen City based on MAXENT. *Progress in Geography*, *41*(10), 1868–1881.

[14] Wagner, P. D., Bhallamudi, S. M., Narasimhan, B., Kumar, S., Fohrer, N., & Fiener, P. (2019). Comparing the effects of dynamic versus static representations of land use change in hydrologic impact assessments. *Environmental Modelling & Software*, *122*, 103987.

[15] da Silva Cruz, J., Blanco, C. J. C., & de Oliveira Júnior, J. F. (2022). Modeling of land use and land cover change dynamics for future projection of the Amazon number curve. *Science of The Total Environment*, *811*, 152348.

[16] Wang, T., Yan, J., & Qiao, H. (2020). Analysis and prediction of land-use change characteristics in Kuala Lumpur, Malaysia. *Bulletin of Soil and Water Conservation*, *40*(5), 268–275.

[17] Pei, L., Chen, C., Dai, J., & Wu, D. (2017). Research on forecast trend of land use and land cover change in Daling River Basin based on Markov Model. *Chinese Journal of Soil Science*, *48*(3), 525–531.

[18] Tian, H., Liang, X., Li, X., Liu, X., Ou, J., Hong, Y., & He, Z. (2017). Simulating multiple land use scenarios in China during 2010-2050 based on system dynamic model. *Tropical Geography*, *37*(4), 547–561.

[19] Yang, Q., & Li, X. (2006). Cellular Automata for simulating land use changes based on Support Vector Machine. *National Remote Sensing Bulletin*, *10*(6), 836–846.

[20] Huang, D., & Huang, J. (2017). Application and research progress of the CLUE-S Model. *Journal of Subtropical Resources and Environment*, *12*(3), 77–87.

[21] Liu, X., Liang, X., Li, X., Xu, X., Ou, J., Chen, Y., Li, S., Wang, S., & Pei, F. (2017). A future land use simulation model (FLUS) for simulating multiple land use scenarios by coupling human and natural effects. *Landscape and Urban Planning*, *168*, 94–116.

[22] Liang, X., Guan, Q., Clarke, K. C., Liu, S., Wang, B., & Yao, Y. (2021). Understanding the drivers of sustainable land expansion using a patch-generating land use simulation (PLUS) model: A case study in Wuhan, China. *Computers, Environment and Urban Systems*, *85*, 101569.

[23] Liu, J., Hu, T., Pan, X., Zhang, D., Zhang, L., & Li, Y. (2018). Simulating coastal wetland changes in Hangzhou Bay using Markov-CLUES coupling model. *Ecology and Environment Sciences*, *27*(7), 1359–1368.

[24] Jiang, X., Duan, H., Liao, J., Song, X., & Xue, X. (2022). Land use in the Gan-Lin-Gao region of middle reaches of Heihe River Basin based on a PLUS-SD coupling model. *Arid Zone Research*, *39*(4), 1246–1258.

[25] Chen, F. (2023). *Study on urban flood risk multi-scenario simulation based on SD-PLUS model and MaxEnt model* [Master's thesis]. Guangzhou University.

[26] Wang, X., Ma, B., Li, D., Chen, K., & Yao, H. (2020). Multi-scenario simulation and prediction of ecological space in Hubei province based on FLUS model. *Journal of Natural Resources*, *35*(1), 230–242.

[27] Li, C., Gao, B., Wu, Y., Zheng, K., & Wu, Y. (2022). Dynamic simulation of landscape ecological risk in mountain towns based on PLUS model. *Journal of Zhejiang A&F University*, *39*(1), 84–94.

[28] Lin, J., He, P., Yang, L., He, X., Lu, S., & Liu, D. (2022). Predicting future urban waterlogging-prone areas by coupling the maximum entropy and FLUS model. *Sustainable Cities and Society*, *80*, 103812.

[29] Xu, N., Song, X., Chen, H., & Xu, C. (2024). Evolution and prediction of waterlogging risk in Nanjing City under the land use changes. *China Rural Water and Hydropower*, (12), 35–42.

[30] Shenzhen Municipality Bureau of Statistics, & Survey Office of the National Bureau of Statistics in Shenzhen. (2023). *Shenzhen Statistical Yearbook 2023*. China Statistics Press.

[31] Meteorological Bureau of Shenzhen Municipality. (2024, May 15). *Climate*

overview and seasonal characteristics of Shenzhen.

[32] He, G. (2019). Experiences and insights from Guangdong Province's flood, drought, and typhoon prevention work in 2018. *China Flood & Drought Management*, *29*(1), 101–103.

[33] Liu, H., Luo, N., & Zhao, Q. (2023). Risk analysis of typhoon disaster chain in Shenzhen based on complex network. *Journal of Catastrophology*, *38*(4), 228–234.

[34] Bureau of Planning and Natural Resources of Shenzhen Municipality. (2019, July 3). *Notice on the publication of the Special Plan and Implementation Scheme for Sponge City Construction in Shenzhen* (Optimized).

[35] Riahi, K., van Vuuren, D. P., Kriegler, E., Edmonds, J., O'Neill, B. C., Fujimori, S., … & Tavoni, M. (2017). The shared socioeconomic pathways and their energy, land use, and greenhouse gas emissions implications: An overview. *Global Environmental Change*, *42*, 153–168.

[36] Wu, T., Lu, Y., Fang, Y., Xin, X., Li, L., Li, W., ... & Liu, X. (2019). The Beijing Climate Center Climate System Model (BCC-CSM): The main progress from CMIP5 to CMIP6. *Geoscientific Model Development*, *12*(4), 1573–1600.

[37] Wang, J., Wu, Y., & Gou, A. (2023). Habitat quality evolution characteristics and multi-scenario prediction in Shenzhen based on PLUS and InVEST models. *Frontiers in Environmental Science*, *11*, 1146347.

[38] Lan, J., & Qu, L. (2024). Multi-scenario simulation of land use and carbon storage assessment in the Pearl River Basin in the next decade. *Journal of Soil and Water Conservation*, *38*(3), 266–275.

[39] Aerts, J. C. J. H., Botzen, W. J. W., Emanuel, K., Lin, N., De Moel, H., & Michel-Kerjan, E. O. (2014). Evaluating flood resilience strategies for coastal megacities. *Science*, *344*(6183), 473–475.

[40] Trenberth, K. E. (2011). Changes in precipitation with climate change. *Climate Research*, *47*, 123–138.

[41] Huang, P.-C. (2022). An effective alternative for predicting coastal floodplain inundation by considering rainfall, storm surge, and downstream topographic characteristics. *Journal of Hydrology*, *607*, 127544.

[42] Gao, J., Holden, J., & Kirkby, M. (2016). The impact of land-cover change on flood peaks in peatland basins. *Water Resources Research*, *52*(5), 3477–3492.

[43] Li, H., Wang, Q., Li, M., Zang, X., & Wang, Y. (2024). Identification of urban waterlogging indicators and risk assessment based on MaxEnt model: A case study of Tianjin Downtown. *Ecological Indicators*, *158*, 111354.

[44] Wang, R., Kalin, L., Kuang, W., & Tian, H. (2014). Individual and combined effects of land use/cover and climate change on Wolf Bay watershed streamflow in southern Alabama. *Hydrological Processes*, *28*(22), 5530–5546.

[45] Ya, R., Wu, J., Tang, R., & Zhou, Q. (2023). Increased flood susceptibility in the Tibetan Plateau with climate and land use changes. *Ecological Indicators*, *156*, 111086.

[46] Warren, D. L., & Seifert, S. N. (2011). Ecological niche modeling in Maxent: The importance of model complexity and the performance of model selection criteria. *Ecological Applications*, *21*(2), 335–342.

[47] Radosavljevic, A., & Anderson, R. P. (2014). Making better Maxent models of species distributions: Complexity, overfitting, and evaluation. *Journal of Biogeography*, *41*(4), 629–643.

[48] Kass, J. M., Muscarella, R., Galante, P. J., Bohl, C. L., Pinilla-Buitrago, G. E., Boria, R. A., Soley-Guardia, M., & Anderson, R. P. (2021). ENMeval 2.0: Redesigned for customizable and reproducible modeling of species' niches and distributions. *Methods in Ecology and Evolution*, *12*(9), 1602–1608.

[49] Yuan, X. (2022). *Scenario simulation of land use change and landscape ecological risk research in Wuhan based on PLUS model* [Master's thesis]. East China University of Technology.

[50] Rezaei, S., Mohammadi, A., Shadloo, S., Ranaie, M., & Wan, H. Y. (2023). Climate change induces habitat shifts and overlaps among carnivores in an arid and semi-arid ecosystem. *Ecological Informatics*, *77*, 102247.

[51] Yan, M., Li, Q., Song, J., Wang, Z., Wang, Y., & Hu, M. (2019). Prediction of potential distribution areas of Chinese horseshoe crab and mangrove horseshoe crab in the Beibu Gulf of Guangxi based on MAXENT model and their population conservation strategies. *Acta Ecologica Sinica*, *39*(9), 3100–3109.

[52] Duan, C., Zhang, J., Chen, Y., Lang, Q., Zhang, Y., Wu, C., & Zhang, Z. (2022). Comprehensive risk assessment of urban waterlogging disaster based on MCDA-GIS integration: The case study of Changchun, China. *Remote Sensing*, *14*(13), 3101.

[53] Dekongmen, B. W., Kabo-bah, A. T., Domfeh, M. K., Sunkari, E. D., Dile, Y. T., Antwi, E. O., & Gyimah, R. A. A. (2021). Flood vulnerability assessment in the Accra Metropolis, southeastern Ghana. *Applied Water Science*, *11*, 134.

[54] Yang, J., & Chu, X. (2013). Quantification of the spatio-temporal variations in hydrologic connectivity of small-scale topographic surfaces under various rainfall conditions. *Journal of Hydrology*, *505*, 65–77.

[55] Chen, X. (2018). *Study on impacts of underlying surface change on the waterlogging in the downtown area of Wuhan* [Master's thesis]. Wuhan University.

https://doi.org/10.15302/J-LAF-0-020040 收稿日期 | 2024-10-19 录用日期 | 2025-03-19 中图分类号 | TU984, TU986 文献标识码 | A

基于MaxEnt–PLUS模型的城市内涝风险预测及影响因素分析

栾博[1,*]，罗珈柠[1]，叶秀林[1]，黄卫东[2]，俞露[2]，于光宇[2]

1 北京大学深圳研究院绿色基础设施研究所，深圳 518057
2 深圳市城市规划设计研究院股份有限公司，深圳 518028

*通信作者
地址：广东省深圳市南山区高新南七道15号
邮编：518057
邮箱：luanbo@pku.edu.cn

摘要

如何科学预测未来城市内涝风险已成为城市规划领域面临的关键问题。作为受台风、风暴潮和极端降雨等气候灾害严重影响的高密度城市，深圳的城市内涝风险不断加剧，亟需有效提升城市韧性。本研究耦合MaxEnt模型和PLUS模型，基于全球气候模式的典型因子，在自然发展、规划引导和生态保护3种发展情景下预测2040年、2060年、2080年和2100年深圳的土地利用变化和内涝风险并识别其影响因素，进而提出城市更新用地优化策略。结果表明，在气温和降雨量上升的长期趋势下，城市建设用地相较于蓝色空间和绿色空间面临更高的内涝风险，而以生态保护情景发展可有效降低城市内涝风险，至2100年，其高风险区面积相较于2020年将下降7.29%，低风险区面积将增加18.79%。同时，研究发现土地利用类型和高程是影响内涝风险主要因素。本研究可为韧性城市建设提供科学依据，为存量城市更新和绿色基础设施优化布局提供支撑。

关键词

城市内涝；MaxEnt–PLUS模型；韧性城市；蓝绿基础设施；气候适应

文章亮点

- 耦合MaxEnt模型和PLUS模型，预测了深圳在3种发展情景下的未来内涝风险
- 在自然发展情景下，2100年时建设用地的大幅增长会导致城市内涝高风险区面积相应增加
- 增加绿色空间可有效降低城市内涝高风险区面积
- 土地利用类型与高程是对内涝风险的贡献度最高的影响因素

基金项目

- 国家自然科学基金项目“海岸带城市绿色空间的韧性驱动机制研究——以粤港澳大湾区为例”（编号：52078004）
- 深圳市科技计划项目“库–河–湾生物栖息修复和生态韧性构建技术研发”（编号：KCXFZ20211020164205009）

编辑 高雨婷，周佳怡